ELSEVIER Nuclear Instruments and Methods in Physics Research B 180 (2001) 105–111

NIM B
Beam Interactions
with Materials & Atoms

www.elsevier.nl/locate/nimb

Thickness effects of water overlayer on its explosive evaporation at heated metal surfaces

Yusheng Dou [a,*], Leonid V. Zhigilei [a,b], Zbigniew Postawa [a,c], Nicholas Winograd [a], Barbara J. Garrison [a]

[a] *Department of Chemistry, The Pennsylvania State University, University Park, PA 16802, USA*
[b] *Department of Materials Science and Engineering, Thornton Hall, University of Virginia, Charlottesville, VA 22903, USA*
[c] *Institute of Physics, Jagellonian University, ul. Reymonta 4, PL-30059, Krakow 16, Poland*

Abstract

Molecular dynamics (MD) simulations have been employed to investigate the effect of the thickness of a water overlayer on the character of its ejection from a heated Au surface. The simulations are performed for five systems differing in the thickness of the water overlayer which was adsorbed on a metal substrate heated to 1000 K. For each system, an explosive evaporation occurs in the part of the water film adjacent to the metal surface and the upper part of the film is pushed off by the generated force. The average maximum temperature of the water film decreases as the film thickness increases. In contrast, the temperature achieved by the fast cooling due to the explosive evaporation shows an inverse trend. The significance of these model calculations to matrix-assisted laser desorption and ionization (MALDI) mass spectrometry is discussed. © 2001 Elsevier Science B.V. All rights reserved.

PACS: 68.10.JY
Keywords: Explosive evaporation; Explosive boiling; Phase explosion; MALDI mass spectrometry; Ice matrix; Water film; Molecular dynamics simulation

1. Introduction

Matrix-assisted laser desorption and ionization (MALDI) mass spectrometry is one of the most intensively used techniques in the analysis of non-volatile biological molecules [1], such as proteins and DNA. In this technique, the molecules of interest, or analytes, are incorporated into a matrix of smaller molecules. The matrix absorbs UV or IR laser irradiation, desorbs and brings the analytes to the mass detector without significant fragmentation. There is a growing interest in exploiting H_2O as a matrix [2–6] because it is the major constituent of most biological tissue. If H_2O functions in this fashion, it might be possible to perform analysis of proteins and other analytes directly from intact frozen cells and tissue. One approach toward this direction is to explore IR irradiation of a H_2O matrix with embedded analytes [6–8]. Alternatively, a metal substrate

---

[*] Corresponding author. Tel.: +1-814-865-0494; fax: +1-814-863-0618.
E-mail address: ysd@chem.psu.edu (Y. Dou).

0168-583X/01/$ - see front matter © 2001 Elsevier Science B.V. All rights reserved.
PII: S0168-583X(01)00403-7

with a frozen aqueous solution of biological molecules could be irradiated by a UV laser. In this later case, Williams and co-workers [2–5] utilized the laser to deposit energy into the metal substrate and induce ejection of the ice/DNA mixture by heat transfer through the interface. The physics of processes occurring at the metal–ice interface is assumed to be the same as observed in high-speed imaging experiments of melanosomes irradiated by a pulsed laser beam [9,10], where bubble formation around adsorbing sites was observed to cause the separation of fluid from the laser heated surfaces.

The processes occurring at the metal–water interface have been investigated by optical reflectance [11] and photoacoustic [12] experimental techniques. Recently, we have performed a series of molecular dynamics (MD) simulations for obtaining a detailed microscopic picture of the events occurring at the metal–H_2O interface [13]. The simulations show that an explosive evaporation of the water overlayer occurs in the region adjacent to the metal surface when the substrate is rapidly heated to 1000 K.

Many parameters affecting these processes, such as the water film thickness, the rate of heating of substrate as well as the maximum temperature attained need to be investigated. In this paper, we present the simulation results for the effect of the thickness of the water overlayer on the processes leading to the separation of the overlayer from a quickly heated Au substrate. Experimentally, mass spectra with a good signal-to-noise ratio were recorded from the sample rim only [2,5,6], indicating the significance of the film thickness effects in MALDI mass spectrometry.

In the first part of this paper, we give a brief description of potential functions and treatments of the long-range interaction used in this study. In the second part of the paper, we present the simulation results for water overlayers adsorbed on a Au(1 1 1) surface. The thickness of the H_2O overlayers modeled here ranged from 1.05 to 8.40 nm.

2. Methodology

A detailed description of the various potential functions used in this work is given elsewhere [13]. Briefly, the potential employed to describe the H_2O–H_2O interaction is the simple point charge (SPC) water potential developed by Berendsen et al. [14]. The electrostatic part of the potential is treated by the force shifting scheme [15] with a cutoff distance of 0.85 nm. The H_2O molecule remains rigid during the simulation. The Au–Au interactions are represented by the molecular dynamics/Monte Carlo corrected effective medium (MD/MC-CEM) potential function for fcc metals [16–18]. Au–H_2O interaction is represented by a modified Spohr function [19]. The Spohr function assumes that the metal surface is rigid. The modified form used in this work allows the metal atoms to move and interact with the water molecules [13].

MD simulations have been performed for five systems. In each system the substrate is modeled by a finite microcrystalline of 792 Au atoms in 9 layers of 88 atoms each. The systems vary by the number of water layers. Namely, the five water overlayers considered are 6 layers (192 molecules), 12 layers (384 molecules), 24 layers (768 molecules), 36 layers (1152 molecules) or 48 layers (1536 molecules). The H_2O films are assembled in the way described below. The H_2O molecules in the first layer have their two O–H bonds at $\sim 109°$ from the Au(1 1 1) surface. Each of the H_2O molecules in the next layer has one O–H bond parallel to the surface normal and one O–H bond directed at the O atom in the first layer to form a hydrogen-bond. This bilayer structure is repeated until the required thickness of water film is achieved. The water overlayers constructed in this way were quenched for equilibrium configurations before any heating of the substrate.

Periodic boundary conditions are applied in the directions parallel to the surface. The velocity Verlet algorithm [20] is used to integrate the equations of motion and the RATTLE constraint scheme [21] is used to maintain the H_2O molecules rigid during the simulations. The time step was set to 1.0 fs according to energy conservation tests.

The metal substrate is heated to ~ 1000 K by the following procedure. The bottom layer atoms remain rigid. The next four layer atoms experience stochastic forces introduced by the generalized Langevin equation (GLE) [22] as well as the forces from the metal–metal interactions. The atoms in the top four layers experience forces from the metal–H_2O interactions as well as forces due to metal–metal interactions. With this heating scheme, the temperature equilibrates within the whole substrate in ~ 3 ps time and then remains at ~ 1000 K during the simulation.

3. Results and discussions

In this section, we present the simulation results for the water overlayer at a quickly heated Au(1 1 1) surface for the five systems. First, pictorial results and their analysis are presented and then kinetic energy development during the course of simulation is examined.

Snapshots taken from the simulations for the five systems at the time when the water films start to separate from the substrate are shown in Fig. 1. Fig. 1(a) shows that for 6 layers, the overlayer is ejected in the form of individual molecules or very small clusters. When the thickness of the water film increases, the material removed takes the form of large clusters or even chunks. In each case, around one layer of molecules remains attached to the Au(1 1 1) surface as the attractive force between water and Au surface is greater than the cohesive force of water. A low-density region forms just above this attached layer in each case

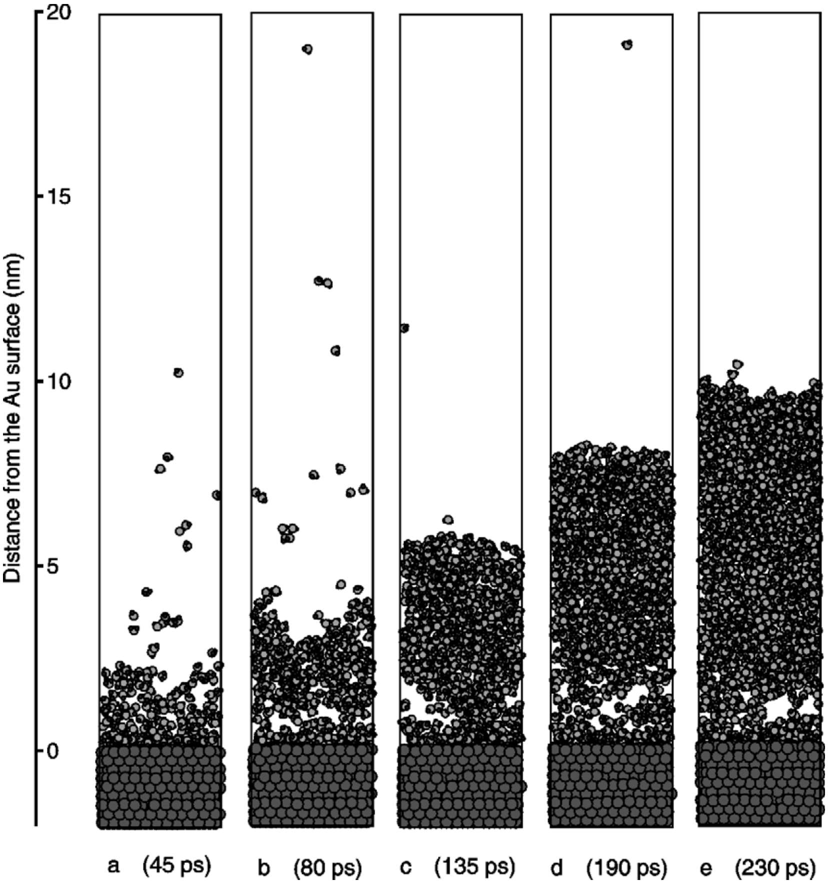

Fig. 1. Snapshots from the MD simulation of water overlayers of different thickness on a Au(1 1 1) surface heated to 1000 K. The overlayer thickness is (a) 6, (b) 12, (c) 24, (d) 36 and (e) 48 water layers. The green, blue and red spheres represent oxygen, hydrogen and gold atoms, respectively.

except the 6-layer system where the molecules readily evaporate from the top of the water film. Time for the onset of film ejection increases from 45 ps for 6 layers to 230 ps for 48 layers.

Snapshots taken from the simulations for the five systems at the time when the main clusters, or chunks are located around 8 nm above the metal surface are shown in Fig. 2. For the 6-layer case, the main cluster is not well defined since only very small clusters are formed. The velocity of the cluster ejection, estimated by examining the time difference between the two snapshots for each system shown in Figs. 1 and 2, decreases as the film thickness increases.

The physics of the ejection was discussed in detail previously [13] and an explosive boiling [23–25] of the region of the water layer adjacent to the metal substrate is found to be the dominant mechanism driving the separation of the overlayer. Essentially, because of fast heating of the metal substrate, the water film just above the Au surface reaches the temperature for explosive evaporation at 500 K. For the thicker film, the top layers are at a lower temperature due to slow thermal conduction. Consequently, an explosive evaporation occurs in the water overlayer nearest to the surface and the outward force pushes off the upper part of the overlayer. Based on this mechanism, the pictorial results presented above can be well understood. The thicker water film needs more time to approach the temperature for explosive evaporation. More layers of water molecules in the thicker

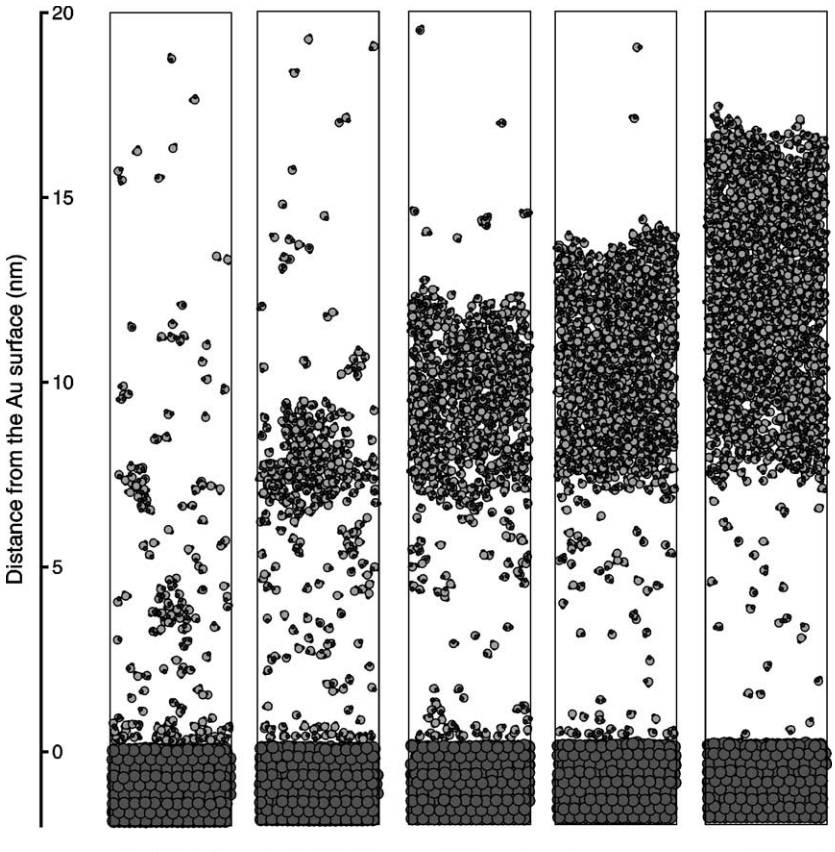

Fig. 2. Same as in Fig. 1 but for later times.

film do not reach the temperature for explosive boiling resulting in the larger clusters being ejected at a lower velocity.

The average temperature and flow kinetic energy for all H_2O molecules versus time for the 6-layer system are shown in Fig. 3. The temperature increases almost linearly until $\sim$ 40 ps when the flow kinetic energy starts to rise. At this time the water film starts to separate from the substrate, as seen from Fig. 1(a). A sharp decline in temperature has been attributed to the fast cooling of ejected material due to the phase explosion [13,25]. In this process thermal kinetic energy is converted into the potential energy for material disintegration as well as the flow kinetic energy. The latter can be confirmed by the fact that a sudden decrease in the radial kinetic energy is accompanied by a steep increase in the flow kinetic energy. The temperature of the water overlayer continuously decreases because of intensive evaporation from the ejected film.

The maximum average temperature of the water film and the final temperature at the end of the simulation versus film thickness are plotted in Fig. 4. Examining the maximum temperature variation first, we find that because the thermal conductivity of the water overlayer is sufficiently slow, the thicker overlayer has a colder upper part and attains a lower average temperature. As a result, the upper part of the film does not undergo explosive boiling and cools by intensive evaporation. This is a slower cooling process than explosive boiling and consequently the thicker film achieves the higher temperature by the end of the simulation.

The simulation results presented above may have important implications for MALDI mass spectrometry. In MALDI, the purpose is to desorb intact analytes. The snapshots presented in Figs. 1 and 2 suggest that thin films may be more effective than thick films at ejecting large molecules. For thin films, the ejection takes the form of individual

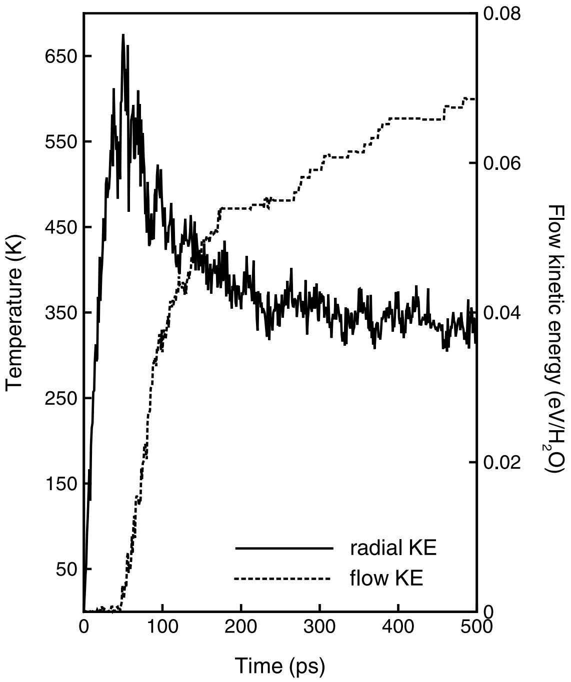

Fig. 3. Temperature and flow kinetic energy versus time for 6-layer system. The temperature has been calculated using only the radial components of the velocity which do not contain the flow component.

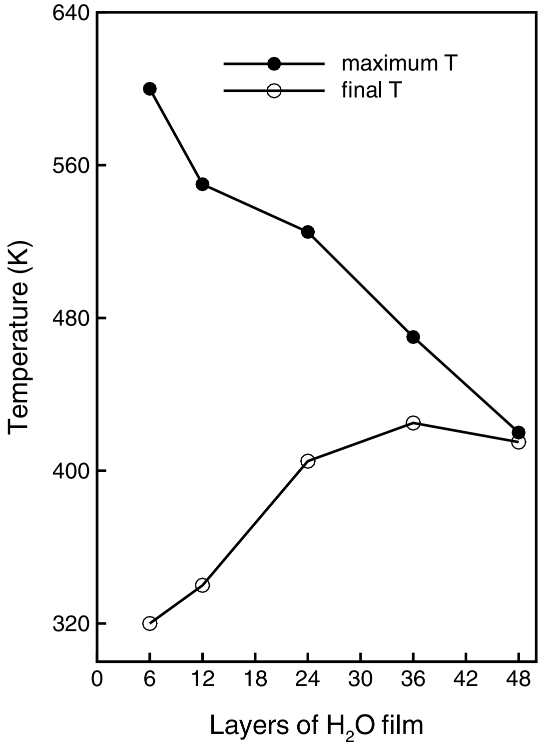

Fig. 4. Maximum and final radial kinetic energies versus the water film thickness.

molecules or very small clusters, allowing an effective volatilization and detection of analytes. For the thicker films, large molecular clusters of water may embed the analyte molecule making it invisible to the detector. The temperature comparison, as shown in Fig. 4, indicates that the thinner film appears to get hotter. The thinner film, however, cools off more rapidly and achieves a lower temperature within a shorter time. It may, therefore, be possible for the analytes to survive the overheating. On the other hand, the maximum temperature of the thick water film is lower than that of the thin film. The temperature of ejected material is still well above the boiling point even after ~ 500 ps of simulation, as shown in Fig. 4 for the 24-, 36- and 48-layer systems. Analytes in the thick films are therefore exposed to a hot environment for a longer time. Faster volatilization of the analytes, that can be expected in the case of the thinner overlayer, would additionally hamper the energy transfer from matrix to analytes and increase the chances for analytes to survive the ejection process. The faster cooling, more efficient volatilization and higher ejection velocity observed for the thin water films make them better candidates for MALDI applications as compared to the thick films.

4. Summary

The MD simulation results performed for the five systems, which differ in the number of the water layers on metal substrate, demonstrate that the thickness of the water film has significant effects on the character of molecular ejection. The thin films eject as individual molecules or very small clusters whereas the thick films yield large clusters or even chunks. The maximum temperature the films experience and the minimum temperature the films reach by the end of the simulation strongly depend on the film thickness. The thin films are heated to the higher temperature than the thick films. However, the thin films undergo faster cooling and consequently achieve lower temperature than the thick films. These results may be important in understanding the experimental conditions in MALDI mass spectrometry using ice as a matrix.

Acknowledgements

The financial support of the National Science Foundation, the National Institute of Health, the Office of Naval Research and the IBM Selected University Research Program are gratefully acknowledged. The Center for Academic Computing at Penn State University provided computational support. ZP would like to acknowledge support from Polish Committee of Scientific Research and NATO CLG grant.

References

[1] D.J. Harvey, Mass Spectrom. Rev. 18 (1999) 349.

[2] R.W. Nelson, W.J. Rainbow, D.E. Lohr, P. Williams, Science 246 (1989) 1585.

[3] R.W. Nelson, R.M. Thomas, P. Williams, Rapid Commun. Mass Spectrom. 4 (1990) 349.

[4] D.M. Schieltz, C.-W. Chou, C.-W. Luo, R.M. Thomas, P. Williams, Rapid Commun. Mass Spectrom. 6 (1992) 631.

[5] P. Williams, Int. J. Mass Spectrom. Ion. Processes 131 (1994) 335.

[6] M. Karas, S. Berkenkamp, F. Hillenkamp, Proc. Natl. Acad. Sci., USA 93 (1996) 7003.

[7] P. Kraft, S. Alimpiev, D. Edward, J. Sunner, J. Am. Soc. Mass Spectrom. 9 (1998) 912.

[8] W. Zhang, S. Niu, B.T. Chait, J. Am. Soc. Mass Spectrom. 9 (1998) 879.

[9] C.P. Lin, M.W. Kelly, Appl. Phys. Lett. 72 (1998) 2800.

[10] C.P. Lin, M.W. Kelly, S.A.B. Sibayan, M.A. Latina, R.R. Anderson, IEEE J. Select. Topics Quantum Electron. 5 (1999) 963.

[11] O. Yavas, P. Leiderer, H.K. Park, C.P. Grigoropoulos, C.C. Poon, W.P. Leung, N. Do, A.C. Tam, Phys. Rev. Lett. 70 (1993) 1830.

[12] H.K. Park, D. Kim, C.P. Grigoropoulos, A.C. Tam, J. Appl. Phys. 80 (1996) 4072.

[13] Y. Dou, L.V. Zhigilei, N. Winograd, B.J. Garrison, J. Phys. Chem. A 105 (2001).

[14] H.J.C. Berendsen, J.P.M. Postma, W.F. van Gunsteren, J. Hermans, in: B. Pullman (Ed.), Intermolecular Forces, Reidel, Dordrecht, 1981.

[15] P.J. Steinbach, B.R. Brooks, J. Comp. Chem. 15 (1994) 667.

[16] M.S. Stave, D.S. Sanders, T.J. Raeker, A.E. DePristo, J. Chem. Phys. 93 (1990) 4413.

[17] T.J. Raeker, A.E. DePristo, Int. Rev. Phys. Che. 10 (1991) 1.

[18] C.L. Kelchner, D.M. Halstead, L.S. Perkins, N.M. Wallace, Surf. Sci. 310 (1994) 425.
[19] E. Spohr, J. Mol. Liq. 64 (1995) 91.
[20] W.C. Swope, H.C. Andersen, P.H. Berens, K.R. Wilson, J. Chem. Phys. 76 (1982) 637.
[21] H.C. Andersen, J. Comput. Phys. 52 (1983) 24.
[22] B.J. Garrison, P.B.S. Kodali, D. Srivastava, Chem. Rev. 96 (1996) 1327 and references therein.
[23] A. Miotello, R. Kelly, Appl. Phys. A 69 (1999) S67.
[24] L.V. Zhigilei, B.J. Garrison, Appl. Phys. Lett. 74 (1999) 1342.
[25] L.V. Zhigilei, B.J. Garrison, J. Appl. Phys. 88 (2000) 1281.